HAMMER TIME

USING THE SCHMIDT HAMMER TO IMPROVE THE FORECASTING ACCURACY OF THE ROCKFALL ACTIVITY INDEX (RAI)

FINAL PROJECT REPORT

by

Daisy M. Herrman and Margaret M. Darrow
University of Alaska Fairbanks

Sponsorship
University of Alaska Fairbanks

for

Pacific Northwest Transportation Consortium (PacTrans) USDOT University Transportation Center for Federal Region 10 University of Washington
More Hall 112, Box 352700
Seattle, WA 98195-2700

In cooperation with U.S. Department of Transportation,
Office of the Assistant Secretary for Research and Technology (OST-R)

DISCLAIMER

The contents of this report reflect the views of the authors, who are responsible for the facts and the accuracy of the information presented herein. This document is disseminated under the sponsorship of the U.S. Department of Transportation's University Transportation Centers Program, in the interest of information exchange. The Pacific Northwest Transportation Consortium, the U.S. Government and matching sponsor assume no liability for the contents or use thereof.

TECHNICAL REPORT DOCUMENTATION PAGE

1. Report No.	2. Government Accession No.	3. Recipient's Catalog No.
	01872753	

4. Title and Subtitle	5. Report Date
HAMMER TIME USING THE SCHMIDT HAMMER TO IMPROVE THE FORECASTING ACCURACY OF THE ROCKFALL ACTIVITY INDEX (RAI)	July 6, 2023
	6. Performing Organization Code

7. Author(s) and Affiliations	8. Performing Organization Report No.
Daisy M. Herrman, Margaret M. Darrow. 0000-0003-4078-4746 University of Alaska Fairbanks	**2022-S-UAF-1**

9. Performing Organization Name and Address	10. Work Unit No. (TRAIS)
PacTrans Pacific Northwest Transportation Consortium University Transportation Center for Federal Region 10 University of Washington More Hall 112 Seattle, WA 98195-2700	**11. Contract or Grant No.** 69A3551747110

12. Sponsoring Organization Name and Address	13. Type of Report and Period Covered
United States Department of Transportation Research and Innovative Technology Administration 1200 New Jersey Avenue, SE Washington, DC 20590	Research, 1/16/2022-4/15/2023
	14. Sponsoring Agency Code

15. Supplementary Notes

Report uploaded to: www.pactrans.org

16. Abstract

The Schmidt hammer is a widely used and inexpensive instrument for estimating rock strength either in the lab or in the field. Our research team tested the accuracy and repeatability of the Schmidt hammer to estimate rock strength on six Alaskan rock slopes and four Washington/Oregon rock slopes. We determined *in situ* rock hardness by using two different Schmidt hammers (Types L and N); conducted unconfined compressive strength (UCS) testing for select Alaskan rock samples; and summarized the advantages and disadvantages of using the Schmidt hammer in the field. Parameters that potentially affect Schmidt hammer results include testing methodology, sample testing conditions, and data reduction. Our results indicated that major structures within a rock unit (such as bedding or foliation), variation in mineralogy, and moisture content will significantly affect Schmidt hammer results. After data collection, several correction methods can be used to process the Schmidt hammer results. The choice of method depends on the intent of the measurements (i.e., strength of the intact rock or the rock mass), and the application of any method can alter the final results. Our UCS results generally correlated to the Schmidt hammer rebound values (e.g., rock types with high rebound values also had high UCS values). Before utilizing the Schmidt hammer, we suggest users determine the final goal before selecting the Schmidt hammer and testing methodology; identify the rock type and potential discontinuities that can influence results; identify the bias in sample or site selection; and select the most applicable data reduction method for the identified goal.

17. Key Words	18. Distribution Statement		
Engineering geology, Schmidt hammer, strength testing			
19. Security Classification (of this report)	**20. Security Classification (of this page)**	**21. No. of Pages**	**22. Price**
Unclassified.	Unclassified.	25	N/A

Form DOT F 1700.7 (8-72) **Reproduction of completed page authorized.**

SI* (MODERN METRIC) CONVERSION FACTORS

APPROXIMATE CONVERSIONS TO SI UNITS				
Symbol	**When You Know**	**Multiply By**	**To Find**	**Symbol**
		LENGTH		
in	inches	25.4	millimeters	mm
ft	feet	0.305	meters	m
yd	yards	0.914	meters	m
mi	miles	1.61	kilometers	km
		AREA		
in^2	square inches	645.2	square millimeters	mm^2
ft^2	square feet	0.093	square meters	m^2
yd^2	square yard	0.836	square meters	m^2
ac	acres	0.405	hectares	ha
mi^2	square miles	2.59	square kilometers	km^2
		VOLUME		
fl oz	fluid ounces	29.57	milliliters	mL
gal	gallons	3.785	liters	L
ft^3	cubic feet	0.028	cubic meters	m^3
yd^3	cubic yards	0.765	cubic meters	m^3
	NOTE: volumes greater than 1000 L shall be shown in m^3			
		MASS		
oz	ounces	28.35	grams	g
lb	pounds	0.454	kilograms	kg
T	short tons (2000 lb)	0.907	megagrams (or "metric ton")	Mg (or "t")
		TEMPERATURE (exact degrees)		
°F	Fahrenheit	5 (F-32)/9 or (F-32)/1.8	Celsius	°C
		ILLUMINATION		
fc	foot-candles	10.76	lux	lx
fl	foot-Lamberts	3.426	$candela/m^2$	cd/m^2
		FORCE and PRESSURE or STRESS		
lbf	poundforce	4.45	newtons	N
lbf/in^2	poundforce per square inch	6.89	kilopascals	kPa

APPROXIMATE CONVERSIONS FROM SI UNITS				
Symbol	**When You Know**	**Multiply By**	**To Find**	**Symbol**
		LENGTH		
mm	millimeters	0.039	inches	in
m	meters	3.28	feet	ft
m	meters	1.09	yards	yd
km	kilometers	0.621	miles	mi
		AREA		
mm^2	square millimeters	0.0016	square inches	in^2
m^2	square meters	10.764	square feet	ft^2
m^2	square meters	1.195	square yards	yd^2
ha	hectares	2.47	acres	ac
km^2	square kilometers	0.386	square miles	mi^2
		VOLUME		
mL	milliliters	0.034	fluid ounces	fl oz
L	liters	0.264	gallons	gal
m^3	cubic meters	35.314	cubic feet	ft^3
m^3	cubic meters	1.307	cubic yards	yd^3
		MASS		
g	grams	0.035	ounces	oz
kg	kilograms	2.202	pounds	lb
Mg (or "t")	megagrams (or "metric ton")	1.103	short tons (2000 lb)	T
		TEMPERATURE (exact degrees)		
°C	Celsius	1.8C+32	Fahrenheit	°F
		ILLUMINATION		
lx	lux	0.0929	foot-candles	fc
cd/m^2	$candela/m^2$	0.2919	foot-Lamberts	fl
		FORCE and PRESSURE or STRESS		
N	newtons	0.225	poundforce	lbf
kPa	kilopascals	0.145	poundforce per square inch	lbf/in^2

*SI is the symbol for the International System of Units. Appropriate rounding should be made to comply with Section 4 of ASTM E380.
(Revised March 2003)

TABLE OF CONTENTS

LIST OF FIGURES

LIST OF TABLES

ACKNOWLEDGMENTS

Our team would like to acknowledge the time and efforts of Dr. Matt Bray, Matthew Encelewski, and Drs. Michael Olsen, Joe Wartman, and Ben Leshchinsky of the “RAI of Data” research team.

EXECUTIVE SUMMARY

The Schmidt hammer is a widely used and inexpensive instrument for estimating rock strength either in the lab or in the field. This indirect testing method can provide rock strength information without destroying the sample like other testing procedures (e.g., unconfined compressive strength (UCS) testing). In collaboration with another PacTrans-funded project (Darrow et al. *In Review*), our research team tested the accuracy and repeatability of the Schmidt hammer to estimate rock strength on six Alaskan rock slopes and four Washington/Oregon rock slopes, all sites of long-term data collection and rockfall analysis. For this project, we 1) determined *in situ* rock hardness and weathering conditions at field sites using two different Schmidt hammers (Types L and N); 2) conducted a comprehensive literature review of up-to-date analyses of strength testing using the Schmidt hammer; 3) conducted UCS testing for select Alaskan rock samples; 4) performed a preliminary statistical analysis of Schmidt hammer results as they relate to varying lithology; and 5) summarized the pros and cons of using the Schmidt hammer in the field.

Our literature review identified several parameters that potentially affect Schmidt hammer results, including testing methodology, sample testing conditions, and data reduction. All of these parameters affect the rebound values' correlation to UCS values. Our results indicated that major structures within a rock unit (such as bedding or foliation), variation in mineralogy, and moisture content will significantly affect Schmidt hammer results. After data collection, several correction methods can be used to process the Schmidt hammer results. The choice of method depends on the intent of the measurements (i.e., strength of the intact rock or the rock mass), and the application of any method can alter the final results.

At the Alaska sites, we collected large rock samples representative of each major lithology from each slope for strength testing. Here we present the UCS results of six of the rock types. The UCS results generally correlated to the Schmidt hammer rebound values (e.g., rock types with high rebound values also had high UCS values).

Based on this research, we suggest considering the following before using the Schmidt hammer:

- The selection of Schmidt hammer type is up to the user. The N-Type is potentially a better candidate for general use because of lower scatter in its results.

- Determine the final goal before using the Schmidt hammer and selecting a testing methodology (i.e., acquiring results representative of the rock mass or the intact rock).
- Before recording any values, identify the rock type and determine potential bedding, foliation, persistent jointing, faults, etc. that can influence results at the testing location.
- Differences in testing environments, for example in the field on *in situ* rock versus in the lab on large samples, may affect results as a result of the bias of sample selection.
- Select the most applicable data reduction method for the Schmidt hammer results. The method used will change the final averaged rebound results.

This report is the initial summary of our results. A comprehensive analysis, including the remaining UCS testing, comparison to point load tests and Schmidt hammer tests on lab samples, and the effect of proximity to discontinuities on Schmidt hammer field measurements, will be included in the first author's Master's thesis.

CHAPTER 1. PROJECT MOTIVATION AND BACKGROUND

1.1. Introduction and Background

Slopes pose a significant hazard to transportation infrastructure and mobility across the Pacific Northwest (PNW) because of the combination of the region's geology, topography, high precipitation rates, and seismicity. Rockfall hazards result in frequent road closures, lane restrictions, infrastructure damage, loss of life, and injuries to motorists, cyclists, and pedestrians. Thus, rockfall directly affects driver safety, mobility, and accessibility for many critical lifelines. Recent PacTrans-supported research by Holtan (2021) documented the significant mobility and economic impacts that rockfall has on major roads across the PNW, including road closures for a month or more and emergency repair costs of over $1 million for large events.

The authors are part of a research team that received PacTrans support in 2020 to modify the rockfall activity index (RAI) to account for rockfall attenuation after earthquakes (Darrow et al. 2022). The RAI can be used as a tool by engineers to understand the relative risk between rock slopes, and which slopes are best-suited for mitigation. The team assessed the efficacy, accuracy, and reliability of the RAI methodology and concluded that the automated morphological mapping is highly reliable but that the activity rates for the morphological classes vary more widely than initially estimated by Dunham et al. (2017). These activity rates, which quantify the "activity "or instability rate of the morphological classes, directly control the RAI mapping of rockfall "hotspots." Our verification and accuracy studies of the RAI suggested that the activity rates are not always consistent, generic values, but instead they vary as a function of geology and rock material properties (e.g., well-indurated, freshly weathered crystalline rocks are less active than softer fine-grained rocks such as siltstones), as well as local climate conditions. In 2021, our research team received additional PacTrans support to improve and refine both the accuracy and the interpretation of the RAI analysis to promote its wider adoption by transportation authorities and consulting engineers in the PNW and across the nation (project title - "*A RAI of Data: Generalizing the Data-Driven Rockfall Activity Index (RAI) Based on Long-Term Observations of Well Characterized Slopes*," hereafter referred to as "*A RAI of Data"* (Darrow et al. - *In Review*)). One element of the "A RAI of Data" project was to modify the procedure to estimate the RAI activity rate based on *in situ* rock strength testing with a Schmidt hammer. The Schmidt hammer is a well-established, widely adopted (Aydin and Basu 2005;

Wang and Wan 2019), and easy-to-use field instrument for assessing rock strength in the field. This "Hammer Time" research (presented here) complements the funded "A RAI of Data" project by measuring the accuracy and repeatability of Schmidt hammer data to determine rock strength and weathering conditions, using sites in Alaska, Washington, and Oregon as case studies; the results complement the RAI procedure to conduct "hotspot" mapping, thus improving the accuracy of the RAI methodology. This research represents a key component of the lead author's Master's thesis.

1.2. Research Approach

Here we detail results from Alaska, Washington, and Oregon sites, where we tested the accuracy and repeatability of Schmidt hammer data to determine rock strength and weathering conditions. The following is a summary of the project tasks.

Task 1: We determined *in situ* rock strength and weathering conditions for Alaska and Washington/Oregon field sites. The selected project areas were the sites of long-term, PacTrans-funded data collection in Alaska (along the Parks Highway near the Nenana River Canyon and the Long Lake area of the Glenn Highway; see Figure 1.1) and four project areas in Washington and Oregon (Hewett Lake, Washington (State Route 14); Eddyville, Oregon (US Route 20); Yellow Creek, Oregon (State Highway 138); and Canyonville, Oregon (Interstate 5); see Figure 1.1). We included a comprehensive literature review of up-to-date analyses of strength testing with the Schmidt hammer, identifying knowledge gaps evident from the literature, and described the methodology used in the field.

Task 2: We conducted unconfined compressive strength (UCS) tests on selected Alaskan rock samples. As this project represents part of a Master's thesis, these tests are ongoing; results presented here are preliminary.

Task 3: We performed a preliminary statistical analysis of the Schmidt hammer results as related to lithology and rock slope classifications. Natural rock is inherently variable, with differences in mineralogy, grain size, microfractures, alteration, and weathering. Depending on its porosity, it also may vary as a result of environmental conditions, such as moisture content. All of these differences were reflected in the variability of the Schmidt hammer results, described through a brief statistical analysis.

Task 4: We summarized the advantages and disadvantages of using the Schmidt hammer in the field, identifying any major concerns with this method. This summary, based on a

comprehensive case study of multiple sites from two vastly different parts of the PNW, provides practitioners with a practical guide to employ this test method as part of the RAI approach.

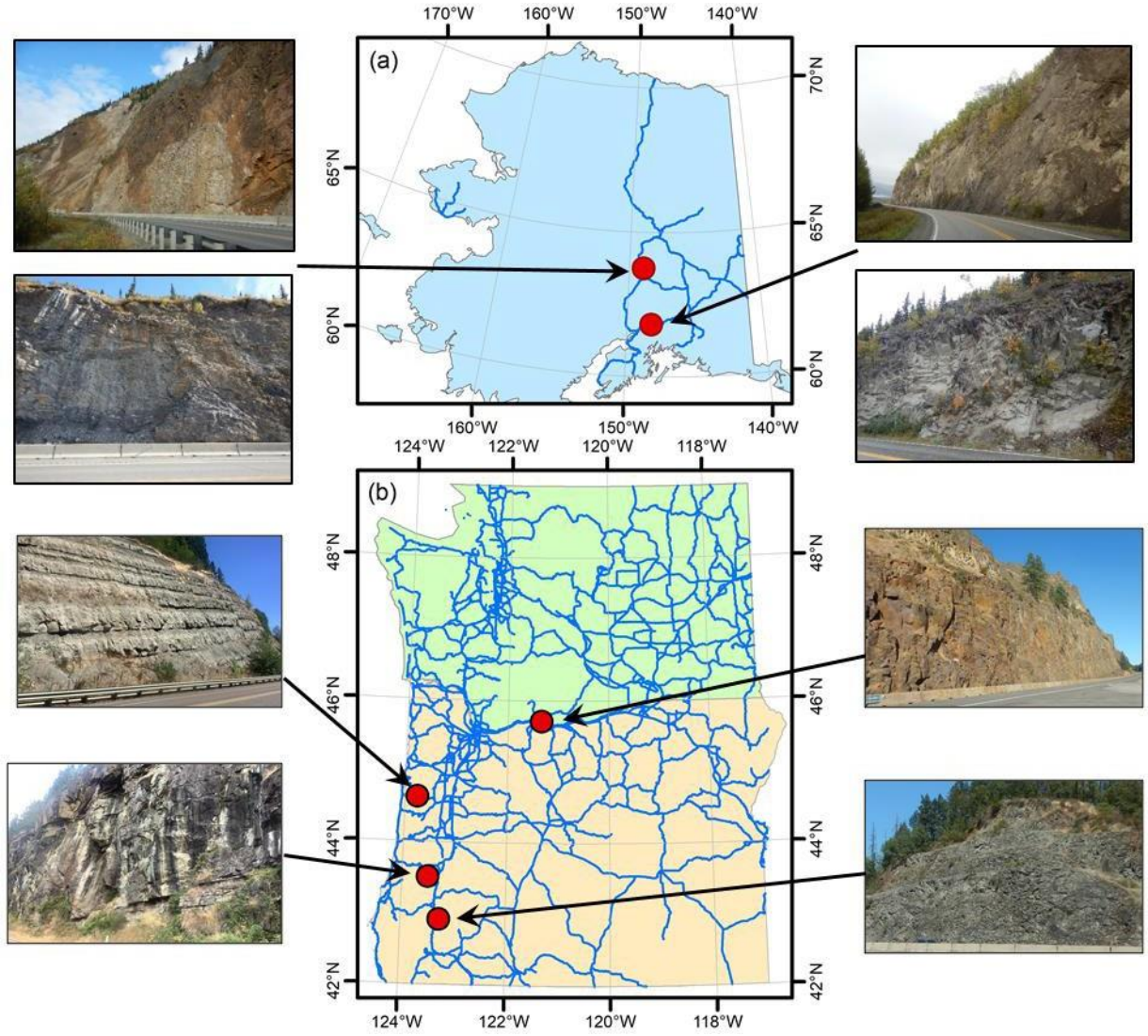

Figure 1.1 Field sites for lidar data collection and rock slope characterization.
(a) ALASKA FIELD SITES: Examples of Nenana Canyon area, Parks Highway (left), and Long Lake area, Glenn Highway (right);
(b) WASHINGTON/OREGON FIELD SITES: counterclockwise from middle right – Hewett Lake, Washington (State Route 14); Eddyville, Oregon (U.S. Route 20); Yellow Creek, Oregon (State Highway 138); Canyonville, Oregon (Interstate 5).
In both map views, blue lines represent major roadways in each state; note that (a) is only a portion of Alaska. Base map imagery from ADOT&PF (2020), AGC (2020), OGEO (2023a and b), WA DNR (2023a and b).

CHAPTER 2. METHODOLOGY

2.1. Literature Review

The Schmidt hammer is a widely used and inexpensive field instrument for quickly estimating rock strength both in the lab and in the field. It is considered an indirect method able to determine rock hardness without destroying the rock sample. There are two types of Schmidt hammers used specifically for rock: N-Type with an impact energy of 2.207 Nm (1.63 ft-lbf) and L-type with an impact energy of 0.735 Nm (0.54 ft-lbf). The Schmidt hammer contains a spring-loaded piston that automatically releases as the plunger is pressed orthogonally against a surface. The impact energy from the piston rebounds through the surface material. Hard materials have a high return measurement, i.e., the piston height after impact, called a rebound value (R). This value is an indication of material hardness, which is correlated to the unconfined compressive strength (UCS).

Our literature review highlighted several aspects of Schmidt hammer testing that need further evaluation. Identified parameters that can affect Schmidt hammer results include testing methodology, sample testing conditions, and data reduction. All of these parameters affect correlation to UCS values. Because there are two types of Schmidt hammers, determining potential variances between them is important because this will inform which hammer is used for a specific rock type. The literature contains differing recommendations for which hammer type is best for rock strength testing. The IRSM (1978) suggested using an L-Type hammer, while the ASTM (ASTM International 2014) did not specify. Aydin and Basu (2005) suggested that using the N-Type hammer will reduce scatter because of its higher impact strength. The rock strength threshold for each hammer is not strictly defined, leading to ambiguity about which device to use. Both hammers can be used to estimate rock strength, but the L-Type may be more accurate for weaker rock (UCS < 10 MPa) whereas the N-Type is more accurate for harder rock (UCS > 10-250 MPa) (Aydin and Basu 2005). Additionally, strict rules have not been established for how many readings are necessary to capture a representative R value. The number of impacts at the testing site can alter measurements and introduce scatter. According to Hucka (1965) and Poole and Farmer (1980), multiple impacts in one spot are more consistent, but Aydin and Basu (2005) indicated that the readings likely represent an altered state of the rock as a result of compaction of the rock surface. One impact can be more representative, but potentially less consistent.

Rock is a heterogeneous material with inherent anisotropy due to varied mineral composition and crystalline structure. Major structures within a rock unit, such as bedding or foliation, can significantly alter the R value, depending on impact orientation. To eliminate some of these variables, researchers conducted Schmidt hammer testing on lab core samples rather than *in situ* rock surfaces (e.g., Aydin and Basu 2005; Wang and Wan 2019), since different testing environments can affect measured rebound values. As indicated by ASTM D5873-14 (ASTM International 2014), lab samples are intact rock specimens free of the major discontinuities, weathering, and alteration that may weaken a natural rock face in the field. Additionally, lab core samples provide a smooth testing surface, eliminating asperities or irregularities that reduce the resulting measurement as a result of energy loss on impact (Aydin and Basu 2005; ASTM International 2014; Wang and Wan 2019). Testing on an *in situ* rock surface may be affected by those variations in the rock mass. Proximity to sample boundaries in the lab and to discontinuities in the field cause low R values (IRSM 1978; ASTM International 2014). Even discontinuities invisible below the surface can reduce R values by dissipating energy and introducing scatter. The IRSM (1978) suggested testing 6 cm (2.36 in.) from the sample edge and major discontinuities, whereas ASTM International (2014) suggested a 15-cm (5.91-in.) distance from the sample edge and 6 cm (2.36 in.) from major discontinuities. Weathering also alters the R value, especially in rock types with coarse-grained minerals as a result of different weathering susceptibilities (Aydin and Basu 2005). Moisture content is another parameter that can vary significantly between lab and field settings. When the moisture content is higher, the rock's compressive strength is lower because of an increase in pore water pressure (Liu et al. 2011).

Data reduction methods to determine a representative R value vary depending on the intention of the study; the strength value can be representative of the intact rock or of the rock mass. The IRSM (1978) recommended averaging the upper 50 percent of 20 single impact readings. ASTM International (2014) suggested taking ten impacts, averaging those ten readings, removing the R values that differ from the average by 7 or more, and then averaging the remaining values. Shorey et al. (1984) recommended taking the lower mean of averaged values, whereas Amaral et al. (1999) recommended taking all values into account. The data reduction method can alter the results significantly, changing the estimated rock strength. The R value by itself can be used as an index of rock hardness, but in most studies, the R values were converted

to UCS through empirical relationships. There is a wide range of empirical formulas, but there is no one universal formula; instead, each is for a specific rock type / strength, hammer type, and R value. Aydin and Basu (2005) provided a summary of empirical formulas, relevant lithologies, rock strength, and R value ranges from several sources.

2.2. Schmidt Hammer Testing Procedure

Before going to the field, we calibrated each hammer by using a Silver Schmidt Calibration Anvil as per the manufacturer's specifications (Proceq 2017). Following the Rock Schmidt Rebound Hammer calibration procedure, ten hits on the anvil per hammer type were performed and then averaged. The average value for each hammer type was within the expected range provided by the manufacturer. If a Schmidt hammer falls out of calibration, a correction factor can be applied to measured values (IRSM 1978). Our team collected field data during two campaigns: June 8-12, 2022, for the Alaska sites; and August 15-19, 2022, for the southern Washington and Oregon sites (Table 2.1). At all sites we collected readings using two Schmidt hammer (SH) devices (Rock Schmidt Rebound Hammer Types N and L) to conduct a systematic comparison for multiple rock types and weathering conditions in a field setting. Two individuals conducted the testing with both hammer types. All SH tests were conducted following ASTM standards (ASTM International 2014) with the exception that we did not use the grinding stone on the *in situ* rock surfaces. Before testing began, we developed a procedure to address the influence of various parameters on the results.

At each site, we identified a minimum of ten SH testing locations along the rock slope face. At each location, we constructed a grid of ten points within a 1-m^2 area (see Figure 2.1a for a grid example). Testing locations were georeferenced by using a Leica GS18 real-time kinematic global positioning system (RTK-GPS) at the Alaska sites, and a combination of Leica GS18 and GS14 rover and base pairs at the Washington and Oregon sites. To address potential user bias, we developed an additional testing grid of ten points (Figure 2.1b) for locations where two individuals took measurements. The distance between each testing point on the grid was greater than 6 cm (2.36 in.) to prevent any overlap of deformation on the rock face. To check for the potential effect of multiple shots and different hammer types, we took a measurement with each hammer type at each point, alternating which hammer type was used first at the different locations. If applicable, we noted the orientation to foliation or bedding because this can affect rebound values. Testing parallel rather than perpendicular to bedding or foliation may cause the

recorded rebound values to be lower because of the dissipation of energy along the bedding or foliation plane. Additionally, at every other SH location we collected a water content sample in a sealed tin and transported these to the University of Alaska Fairbanks (UAF) for testing.

Table 2.1 Summary of Schmidt hammer testing sites

Name	Abbreviation	Highway	State	Rock type(s)
Long Lake MP71	LL71	Glenn Highway	AK	mudstone
Long Lake MP75	LL75	Glenn Highway	AK	rhyodacite, sandstone
Long Lake MP85.5	LL85.5	Glenn Highway	AK	gabbro
Long Lake MP87	LL87	Glenn Highway	AK	sandstone
Nenana Canyon MP239	NC239	Parks Highway	AK	diabase; schist unit consisting of white mica schist, muscovite sericite schist, and quartzite
Nenana Canyon MP241	NC241	Parks Highway	AK	quartzite
Hewett Lake	HL	State Route 14	WA	basalt
Eddyville	EDE	U.S. Route 20	OR	sandstone, siltstone
Yellow Creek	YC	State Highway 138	OR	sandstone, siltstone
Canyonville	CNM	Interstate 5	OR	tuff

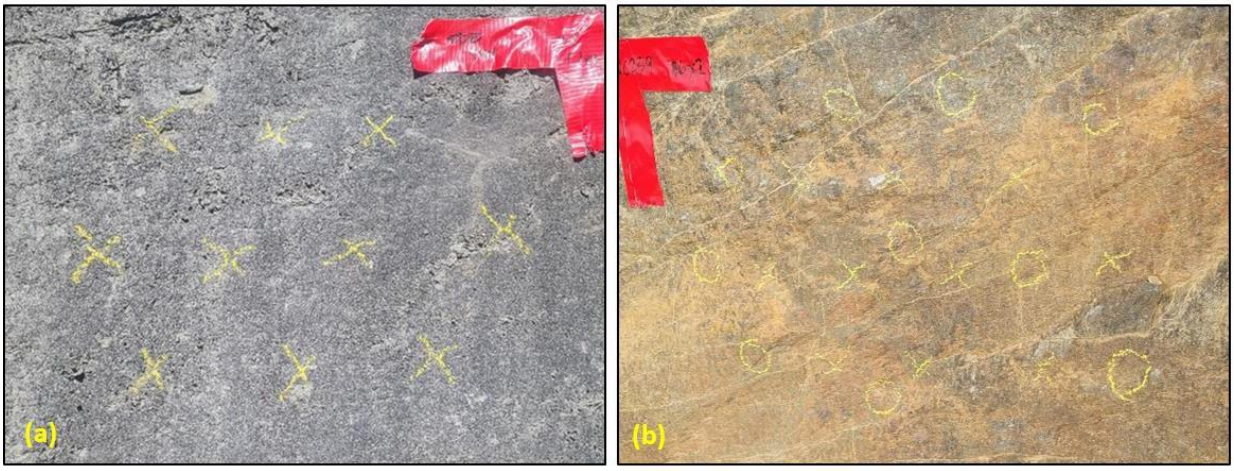

Figure 2.1 Examples of Schmidt hammer (SH) testing locations: (a) a grid set-up on the slope face (yellow X's indicate impact locations) used for standard and "Super Sites" tested by one individual; (b) a grid set-up for two individuals taking measurements (indicated by yellow X's and O's).

We established additional SH testing locations on the rock face to determine the effects of repeated impacts from the SH—we called these locations "Super Sites" (SS). At these

locations, we measured a grid of ten testing points using only one hammer type; we alternated hammers between SS testing sites. On each point in the grid, we measured ten consecutive R values. These locations were used to determine possible changes to rebound measurements with successive impacts.

2.3. Unconfined Compressive Strength (UCS) Testing

2.3.1. Sample Collection and Preparation

At the Alaska sites, we collected large rock samples representative of each major lithology from each slope and transported them to the Geological Engineering laboratory at UAF for sample preparation for strength testing (Figure 2.2). Large rocks were selected on the basis of their dimensions and lack of discontinuities to ensure ample material for laboratory testing.

Figure 2.2 View of rock specimens (within yellow ellipse) transported in the back of a pick-up truck for strength testing.

For competent rock blocks (i.e., the LL75 rhyodacite and NC239 diabase), we prepared five cylindrical core samples according to the ASTM D7012 standard, Method C, which requires a minimum required diameter of 57 mm (2.24 in.) (ASTM International 2014). We used a 5.08-cm (2-in.) diameter coring bit and trimmed each core to a length of 10.16 cm (4 in.) to obtain the

2:1 length-to-diameter ratio per the ASTM specifications (ASTM International 2014) (see Figure 2.3a).

Because of the prominent bedding, foliation, and jointing within the LL71 mudstone, LL75 and LL87 sandstone, LL85 gabbro, and NC schist units, none of these rocks would produce an intact core sample. Therefore, we took an alternative approach to make UCS samples from these rock types. Du et al. (2019) and Durmekova et al. (2021) indicated that cylindrical samples with a length-to-diameter ratio of 2:1 and prism samples with a length-to-width ratio of 2:1 yielded similar results, with only minor differences in UCS strength between the two specimen shapes. Instead, these authors found that decreasing the length-to-width ratio had a more significant effect on the strength results, typically causing them to increase.

Therefore, we prepared prism samples for the rock types that would not produce cores. First, we cut slabs of rock with a large masonry saw. Using a smaller saw, we cut the slabs precisely to the dimensions of 10.16 cm x 5.08 cm x 5.08 cm (4 in. x 2 in. x 2 in.) (Figure 2.3b); to maintain consistency with the cylindrical samples, we used a length-to-width ratio of 2:1.

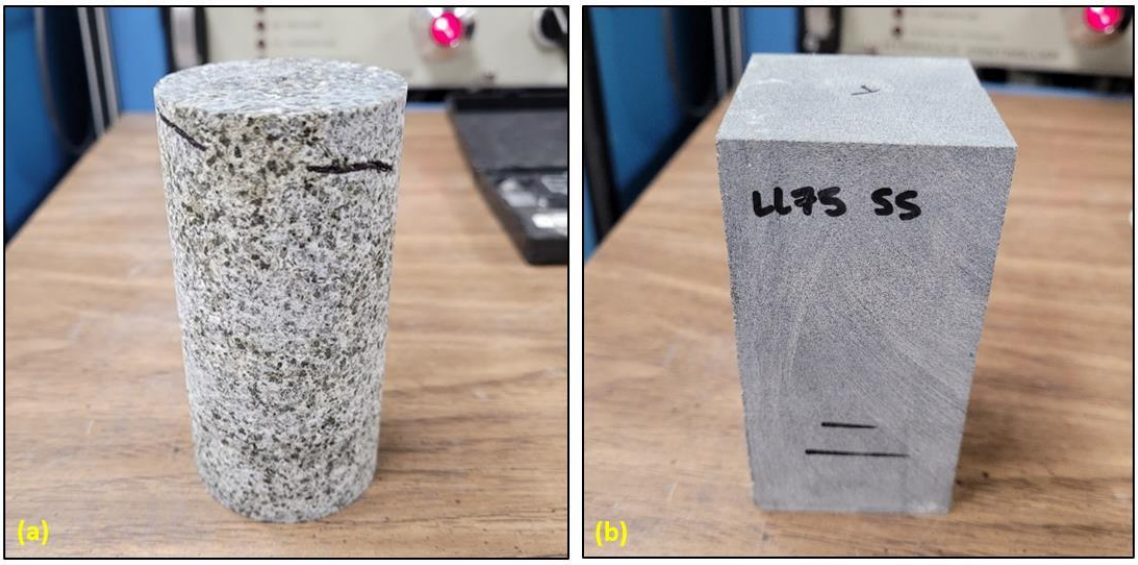

Figure 2.3 Images of (a) cylindrical and (b) prism samples before strength testing. Prominent discontinuities are marked on each sample in black.

We ground the loading surfaces of each sample level to within a 0.02-mm (0.000787-in.) tolerance with a grinder. Before testing, we collected length, width, and diameter measurements (± 0.00127 cm / 0.0005 in.) and mass measurements (± 0.05 g / 0.00011 lb). Images were taken

of each sample, in which we indicated the locations of prominent discontinuities, crystals, and veins (larger than 10 mm or 0.39 in.; see Figure 2.3). For the LL75 and LL87 sandstone, samples were prepared and tested perpendicular or parallel to bedding to match the field orientation tested by the SH.

Since the NC239 diabase was the most competent rock that we collected, we produced a combination of cylinders (five samples) and prisms (three samples) from this rock type to determine whether the sample's shape had a significant effect on strength results. We could only produce one cylindrical core from the LL85.5 gabbro unit, so we also tested a combination of the two sample shapes for this rock type. Unfortunately, the LL71 mudstone did not provide any viable samples for UCS testing (see Figure 2.4).

Figure 2.4 Examples of the LL71 mudstone behavior during sample preparation: (a) prominent bedding caused the rock to break apart into sheets of varying thickness; (b) an attempt to core a mudstone rock resulted in failure along the bedding and the disintegration of the sample.

2.3.2. Testing Procedure

For UCS testing, we used a heavy-duty load frame suitable for testing high-strength rock cores. Before testing, we cleaned all platens within the testing chamber. After placing the sample in the load frame (Figure 2.5), we loaded it at a continuous rate of 0.000635 cm/s (0.00025 in./s). We selected this loading rate to ensure that the sample would fail within 2 to 15 minutes.

Throughout the testing duration, the testing system recorded load and deformation, and produced a stress-strain diagram graphing the failure process. The UCS was calculated from the

maximum recorded load and the cross-sectional area of the specimen. The failure mode of the sample was noted based on the marked discontinuities and the failure plane angle.

Figure 2.5 Cylindrical rock sample loaded into the UCS testing machine.

CHAPTER 3. RESULTS

3.1. Schmidt Hammer (SH) Data

At the Alaska locations we took 3,050 SH measurements along seven slopes, and at the Oregon and Washington locations we took 1,750 SH measurements along four slopes. Table 3.1 contains the averages of both the unreduced SH values, and those obtained by applying the ASTM D5873-14 methodology (ASTM International 2014). The results were comparable within the calculated standard deviations. The LL75 rhyodacite unit demonstrated the highest averaged unreduced and reduced R values of all sites, with the L-type and N-type hammers both providing an unreduced value of 56 and a reduced value of 55. The Eddyville (EDE) and Yellow Creek (YC) siltstones had the lowest average R values of 0 and 2, respectively. These siltstones also had the highest gravimetric water contents of 8.18 percent for the EDE and 1.94 percent for the YC. For all sites, applying the ASTM data reduction method lowered the standard deviation of the measurements; however, the reduced average R values did not significantly change and were within ± 3 of the original averaged R values.

3.2. UCS Testing Results

Of the 11 rock types tested with the SH at the Alaska locations, we prepared samples of seven rock types for strength testing. As mentioned previously, the LL71 mudstone was not viable for UCS testing because of a lack of intact cores or prisms. Additionally, we were not able to test the NC239 / NC241 quartzite before submission of this report because of a breakage within the UCS testing equipment. Table 3.2 contains the UCS results for the seven tested rock types.

To compare results based on sample shape, we tested both cylinders and prisms (five of each shape) of the diabase. Because we were unable to produce ample cylinders of the gabbro, we only tested one cylinder and four prisms of this rock type. The diabase provided average UCS values of 191.4 MPa (27,760.2 psi) and 176.2 MPa (25,555.6 psi) for the cylinder and prism samples, respectively. The gabbro UCS results were 113.9 MPa (16,519.8 psi) for the cylinder core and 156.3 MPa (22,669.4 psi) for the prisms. The LL75 sandstone provided the highest average rock strength of 248.9 MPa (36,099.9 psi). The LL87 sandstone was the weakest rock tested with a UCS of 39.3 MPa (5,704.1 psi).

Table 3.1 Summary of SH results and moisture content for all field sites; '---' indicates not tested.

Field site	No. of testing locations (No. of SS)	Rock type	Avg. R, L type (std. dev.)		Avg. R, N type (std. dev.)		Avg. gravimetric moisture content (%)
			All values	ASTM method	All values	ASTM method	
Long Lake (MP71)	10	Mudstone	29 (13.4)	29 (10.4)	31 (14.9)	31 (12.0)	0.66
Long Lake (MP75)	10	Rhyodacite	56 (11.5)	55 (8.3)	56 (11.5)	55 (6.4)	0.68
	10	Sandstone	49 (13.6)	50 (9.0)	52 (12.9)	52 (8.9)	0.89
Long Lake (MP85)	10	Gabbro	51 (14.8)	51 (9.8)	51 (12.6)	51 (7.1)	0.51
Long Lake (MP87)	10	Sandstone	32 (13.2)	31 (11.7)	34 (11.1)	34 (8.2)	1.47
	2	Mudstone	44 (7.9)	43 (3.0)	44 (6.7)	45 (1.5)	---
	2	Basal conglomerate	36 (15.8)	36 (16.5)	36 (10.7)	38 (5.6)	---
	15 (4)	Quartzite	40 (21.9)	40 (18.2)	37 (21.1)	36 (16.1)	0.30
Nenana Canyon (MP239)	11 (2)	Diabase	40 (23.2)	42 (17.7)	40 (24.3)	40 (18.3)	0.47
	2 (2)	White mica schist	39 (16.6)	36 (6.2)	42 (14.8)	43 (2.4)	0.36
Nenana Canyon (MP241)	10 (4)	Quartzite	41 (17.4)	42 (10.6)	42 (17.4)	42 (12.7)	0.14
Hewett Lake	10 (4)	Basalt	53 (13.7)	54 (9.7)	54 (14.8)	55 (8.6)	0.77
Eddyville Yellow Creek	12 (4)	Sandstone	37 (12.7)	38 (11.8)	35 (12.5)	35 (11.7)	1.52

2		0 (0)	0 (0)	1 (3.2)	0 (0)	8.18	
	10 (4)	Sandstone	43 (12.3)	43 (7.4)	41 (12.6)	42 (9.8)	1.14
Siltstone	1	Siltstone	2 (4.7)	0 (0)	2 (5.1)	0 (0)	1.94
Canyonville	11 (4)	Tuff	28 (22.6)	31 (18.2)	28 (22.9)	29 (18.9)	0.47

Table 3.2 Summary of results from the UCS tests.

Field site	Rock type	Core type	Avg. strength (MPa)
LL75	Rhyodacite	Cylinder	227.2
	Sandstone	Prism	248.9
LL85	Gabbro	Cylinder	113.9
		Prism	156.3
LL87	Sandstone	Prism	39.3
NC239	Diabase	Cylinder	191.4
	Diabase	Prism	176.2
	White mica schist	Prism	43.2
	Muscovite sericite schist	Prism	42.2

CHAPTER 4. SUMMARY AND ADVANTAGES AND DISADVANTAGES OF THE SCHMIDT HAMMER

Through this comprehensive study of multiple field sites, we found the SH to be a convenient and effective device. It is a versatile tool that can be applied in both lab and field settings. In the field, the SH is easy to use and inexpensive to implement because the device is hand-held and light-weight. Taking a rebound measurement is straightforward and does not require extensive training to be done correctly. Results from the SH are immediate and require little preparation. This method is nondestructive and will typically leave the *in situ* rock face or sample intact, unlike other types of strength testing. The SH can be applied to rock types that include major discontinuities, unfavorable bedding, and other limitations that prevent the rock from providing ample samples for other types of strength testing (such as UCS).

Through our literature review, we identified several parameters that can affect SH results, including testing methodology, sample testing conditions, and data reduction. In an attempt to determine the effects that these parameters may have on SH results, we developed a procedure to address each. Depending on the rock type, there can be differences in rebound measurements, depending on testing orientation to bedding or foliation. For example, the increased surface roughness when testing parallel to bedding or foliation may contribute to lower rebound measurements. We expected higher SH measurements orthogonal to bedding and foliation, and lower R values parallel to these discontinuities. The LL75 sandstone R values were measured with the impact perpendicular to bedding, whereas the LL87 sandstone R values were measured parallel to bedding. The average ASTM SH LL75 rebound values were 50 (L- type) and 52 (N-type), while the LL87 R values were lower at 31 (L-type) and 34 (N-type). While these differences may have been due to the orientation of the SH testing, they also may have been due to differences in moisture content and/or inherent differences in rock strength between the two different sandstone units.

Because the SH can be used in a variety of environments, this can have a potential effect on R values. For the purpose of this report, we conducted only field SH measurements directly on the slope face. Field locations have discontinuities that may reduce overall rock strength (e.g., prominent jointing, bedding, foliation, etc.), which can translate into lower SH rebound values. The LL87 sandstone had the lowest results for both the SH and UCS testing. As previously mentioned, this unit had the highest water content and was tested parallel to bedding, both of which may have contributed to the lower values. Generally, the SH results can be correlated to rock strength, where

high SH readings indicate high UCS values, but our results did not yield a perfect correlation. The three strongest rock types from the UCS testing—LL75 rhyodacite, LL75 sandstone, and LL87 gabbro—were also the three rock types that had the highest SH readings. While the rhyodacite had the highest average SH value, it did not have the highest measured UCS. The sandstone unit with the third highest SH value resulted in the highest UCS. SH results will vary across the rock mass as a result of the inherent heterogeneity of rock, but they can vary significantly because of differences in crystalline structure, especially in rocks with varied mineral composition. We observed this in the quartzite and schist of NC239, where rebound values varied significantly based on the presence or absence of large quartz veins prevalent in the unit. Some SH test points within the grid measured higher or lower in accordance with higher or lower visible quartz vs. mica content, and these variations were evident in the increased standard deviation for the schist unit (> 15).

Another potential issue is determining which hammer type to use, especially as there is no definitive guidance on their use for rock strength testing. Several references point to L-type hammers as the preferred type for rock strength testing, most likely because this type was identified in the IRSM standard. Other authors have suggested using the N-type because it gives less scatter and works for a large range of rock strengths. According to Ozbek et al. (2017), N-type rebound values are typically higher than L-type values by ~20 to 25 percent. Our rebound results were closer than anticipated, with minimal deviation from each other (± 3). Although the averaged results were similar, the N-Type generally had a lower standard deviation (within ± 3) than the L-Type for all values averaged. This trend also was present with the application of the ASTM data reduction method.

After data collection, choosing the data reduction methodology can impact results. There are several methods to average SH data, the choice of which largely depends on the goal of the study. If the goal is a representative R value for the competent rock mass, then the ASTM and IRSM methods specify retaining the higher rebound values. In contrast, Amaral et al. (1999) suggested keeping all values, with an emphasis on understanding variance sources. Applying the ASTM data reduction method to our data resulted in a decrease in the standard deviation through the removal of outlier measurements. The ASTM average can be considered a rebound value representative of the competent and intact rock mass, where values affected by discontinuities are removed. When all values are averaged, the standard deviation is higher. For our data, the largest increase occurred for the white mica schist, where the standard deviation for the L-type increased from 6.2 with the ASTM method to 16.6 with all values included.

We suggest considering the following before using the SH:

- Based on our results, the selection of SH type is up to the user. The N-Type is potentially a better candidate for general use because of lower scatter in its results.
- Determine the final goal before using the SH and selecting a testing methodology (i.e., acquiring results representative of the rock mass or the intact rock).
- Before recording any values, identify the rock type and determine potential bedding, foliation, persistent jointing, faults, etc. that can influence results at the testing location.
- Differences in testing environments, for example in the field on *in situ* rock versus in the lab on large samples, may affect results because of the bias of sample selection.
- Select the most applicable data reduction method for the SH results. The method used will change the final averaged rebound results.

Finally, this report is the initial summary of our results. A comprehensive analysis, including the remaining UCS testing, comparison to point load tests and SH tests on lab samples, and the effect of proximity to discontinuities on SH field measurements, will be included in the first author's Master's thesis.

CHAPTER 5. REFERENCES

Alaska Department of Transportation and Public Facilities (ADOT&PF), 2020. Alaska DOT&PF Route Centerlines. Fairbanks, Alaska Department of Transportation and Public Facilities. Available from: < https://dot.alaska.gov/stwddes/gis/shapefiles.shtml>

Alaska Geospatial Council (AGC), 2020. Alaska Coastline Shapefiles. Fairbanks, Alaska Geospatial Office. Available from: < https://gis.data.alaska.gov/search?q=alaska%20boundary >

Amaral, P.M., Rosa, L.G., Fernandes, J.C., 1999. "Determination of Schmidt rebound hardness consistency in granite*." Int. J. Rock Mech. Min. Sci*. 36. 833 – 837.

ASTM International, 2014. Standard Test Method for Determination of Rock Hardness by Rebound Hammer Method, D5873-14: ASTM International, West Conshohocken, PA, 6 p.

Aydin, A. and Basu, A., 2005. "The Schmidt hammer in rock material characterization." *Engineering Geology*: 81(1), 1-14, https://doi.org/10.1016/j.enggeo.2005.06.006

Darrow, M. M., Herrman, D. M., Holtan, K, Leshchinsky, B., Olsen, M., Wartman, J., 2022. *The Long-Term Effect of Earthquakes: Using Geospatial Solutions to Evaluate Heightened Rockfall Activity on Critical Lifelines*: PacTrans, Seattle, WA, 74 p.

Darrow, M. M., Herrman, D. M., Leshchinsky, B., Olsen, M. J., Wartman, J., In Review. *A RAI of Data: Generalizing the Data-Driven Rockfall Activity Index (RAI) Based on Long-term Observations of Well- Characterized Slopes*: PacTrans, Seattle, WA, 46 p.

Du, K., Su, R., Tao, M., Yang, C., Momeni, A., Wang, S., 2019. "Specimen shape and cross-section effects on the mechanical properties of rocks under uniaxial compressive stress." *Bulletin of Engineering Geology and the Environment*. 78. 6061-6074.

Dunham, L., Wartman, J., Olsen, M.J., O'Banion, M.S., Cunningham, K., 2017. "Rockfall Activity Index (RAI): a Lidar-derived, morphology-based hazard assessment system." *Eng. Geo.*: 221, 184-192, doi:10.1016/j.enggeo.2017.03.009

Durmekova, T., Bednarik, M., Dikejova, P., Adamcova, R., 2021. "Influence of Specimen Size and Shape on the Uniaxial Compressive Strength Values of Rocks." *Environmental Earth Sciences*. https://doi.org/10.21203/rs.3.rs-670782/v1

Holtan, K., 2021. *Assessing Seismic Rockfall Impacts on Mobility in Transportation Corridors*. MS Thesis, Oregon State University.

Hucka, V., 1965. "A rapid method of determining the strength of rocks in situ." *International Journal of Rock Mechanics and Mining Sciences and Geomechanics Abstracts.* 2. 127-134. https://doi.org/10.1016/0148-9062(65)90009-4.

ISRM, 1978. "Suggested methods for determining hardness and abrasiveness of rocks." *International Journal of Rock Mechanics and Mining Sciences and Geomechanics Abstracts.* 15. 89 – 97.

Liu, X., Shen, J., Liang, L., Han, L., Liu, H., 2011. "Effects of pore pressure on rock strength properties." *Yanshilixue Yu Gongcheng Xuebao/Chinese Journal of Rock Mechanics and Engineering*. 30. 3457- 3563.

Oregon Geospatial Enterprise Office (OGEO), 2023a. Oregon Highway Network. Oregon Geospatial Enterprise Office. Available from: < https://www.oregon.gov/geo/pages/sdlibrary.aspx >

Oregon Geospatial Enterprise Office (OGEO), 2023b. Oregon Area Commissions on Transportation - 2010. Oregon Geospatial Enterprise Office. Available from:< https://www.oregon.gov/geo/pages/sdlibrary.aspx >

Ozbeck, A., Gul, M., Karacan, E., Alca, O., 2017. "Anisotropy effect on strengths of metamorphic rocks." *Journal of Rock Mechanics and Geotechnical Engineering*. 10. 164-175

Poole, R. and Farmer, I., 1980. "Consistency and repeatability of Schmidt Hammer rebound data during field testing." *International Journal of Rock Mechanics and Mining Sciences and Geomechanics Abstracts.* 17. 167-171. https://doi.org/10.1016/0148-9062(80)91363-7.

Proceq, 2017. *Rock Schmidt Operating Instructions*. Proceq. Switzerland.

Shorey, P.R., Barat, D., Das, M.N., Mukherjee, K.P., Singh, B., 1984. Schmidt hammer rebound data for estimation of large scale in situ coal strength. *Int. J. Rock Mech. Min. Sci.,* Geo-mech. Abstr. 21, 39 – 42.

Wang, M. and Wan, W., 2019. "A new empirical formula for evaluating uniaxial compressive strength using the Schmidt hammer test." *International Journal of Rock Mechanics and Mining Sciences*: 123, 104094, https://doi.org/10.1016/j.ijrmms.2019.104094

Washington State Department of Transportation Geospatial Open Data Portal. Available from:< https://data-wadnr.opendata.arcgis.com/search?groupIds=eee2501342024deaaa41a61c48321d42 >

Washington State Department of Natural Resources (WA DNR), 2023a. WA_State_Boundary.

Washington State Department of Natural Resources (WA DNR), 2023b. WSDOT – State Route Line (1:24K) 2012. *Washington State Department of Transportation Geospatial Open Data Portal*. Available from: < https://gisdata-wsdot.opendata.arcgis.com/ >